

ORBITS OF BLACK HOLES IN TRIAXIAL POTENTIALS

Juan Barbosa

Jaime Forero
Advisor

Departamento de Física
Facultad de Ciencias
Universidad de los Andes

OVERVIEW

1 INTRODUCTION

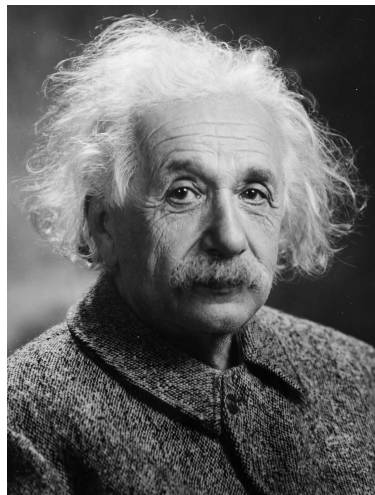
2 METHODOLOGY

- Units
- Equation of motion

3 STUDIES

- Symmetrical
 - Results
- Triaxial
 - Results

INTRODUCTION



- Theory of General Relativity, 1906
- Although more than 100 years have passed since the publication of the theory, even today there are gaps in the understanding and implications of Einstein's equations

└ INTRODUCTION

INTRODUCTION

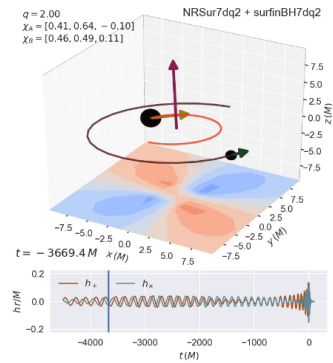


FIGURE: Binary black hole explorer

OBJECTIVES

Study the effect of different triaxial potentials, initial speeds and numerical integrators on the times required by a supermassive black hole to return to its initial position, after experiencing a recoil, as well as to quantify how chaotic its trajectory is.

- Obtain probability distributions for the return times based on each of the free parameters of the triaxial potential, the magnitude and direction of the initial velocity
- Quantify how chaotic is the trajectory of the black hole in each simulation, using exponents of Lyapunov
- Evaluate the performance of the numerical integrators using the information of the simulations

GALACTIC SETUP

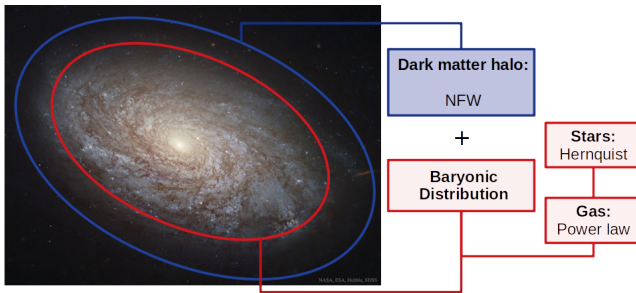


FIGURE: NGC4414 galaxy as seen by the Hubble telescope.

1 Dark matter (NWF):

$$\rho_{\text{DM}}(r) = \frac{\rho_0^{\text{DM}}}{\frac{r}{R_s} \left(1 + \frac{r}{R_s}\right)^2} \quad (1)$$

2 Stellar density (Hernquist):

$$\rho_s(r) = \frac{f_s f_b M_h \mathcal{R}_s}{2\pi r (r + \mathcal{R}_s)^3} \quad (2)$$

3 Gas density (Power law):

$$\rho_{\text{gas}}(r) = \begin{cases} \rho_0^{\text{gas}} & \text{if } r < r_0 \\ \rho_0^{\text{gas}} \left(\frac{r_0}{r}\right)^{-n} & \text{if } r \geq r_0 \end{cases} \quad (3)$$

METHODOLOGY

Mass distributions of the host galaxy, are divergent. The end of the host is taken at the virial radius.

$$\rho_{\text{crit}} = \frac{3H(t)^2}{8\pi G} \quad (4)$$

$$\frac{M(R_{\text{vir}})}{V(R_{\text{vir}})} = \bar{\rho}(R_{\text{vir}}) = 200\rho_{\text{crit}} = 75 \frac{H(t)^2}{\pi G} \quad (5)$$

where $M(R_{\text{vir}})$ is the cumulative mass, and $V(R_{\text{vir}})$: the volume

└ METHODOLOGY

└ UNITS

TABLE: Units of measure used on the simulations.

Physical property	unit
Length	1 kilo-parsec (kpc)
Mass	10^5 solar masses ($10^5 M_\odot$)
Time	1 giga-year (Gyr)

1 Universal gravitational constant:

$$G = 0.4493 \frac{\text{kpc}^3}{\text{Gyr}^2 10^5 M_\odot} \quad (6)$$

2 Hubble parameter:

$$H \approx 1.023 H_0 \times 10^{-3} \text{ Gyr}^{-1} = 6.916 \times 10^{-2} \text{ Gyr}^{-1} \quad (7)$$

└ METHODOLOGY

 └ EQUATION OF MOTION

EQUATION OF MOTION

Trajectories of the kicked black holes are obtained by numerically solving the equation of motion.

$$\ddot{\vec{x}} = -a_{\text{grav}}(\vec{x})\hat{x} + \left(a_{\text{DF}}(\vec{x}, \dot{\vec{x}}) - \dot{x} \frac{\dot{M}_\bullet(x, \dot{x})}{M_\bullet} \right) \dot{\hat{x}} \quad (8)$$

where M_\bullet is the black hole mass

- Dark matter, stars and gaseous materials from the medium interact with the black hole adding a drag force.
- The black hole accretes matter from the surroundings

└ STUDIES
└ SYMMETRICAL

RESULTS

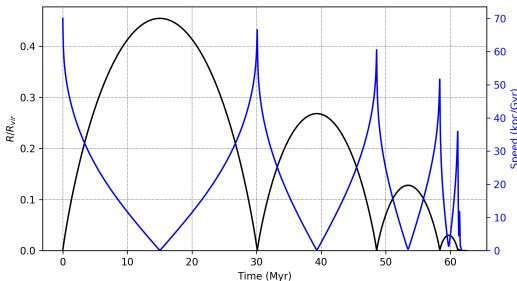
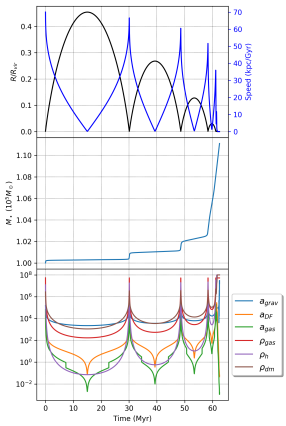


FIGURE: Distances and speeds.

RESULTS

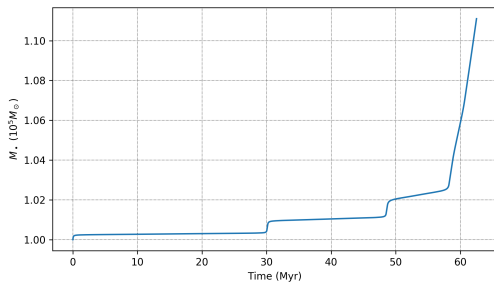
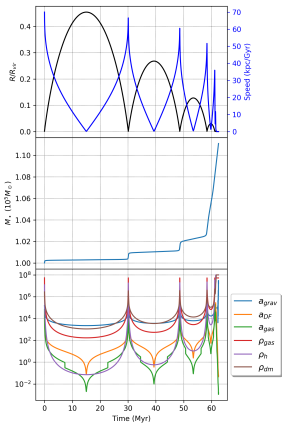


FIGURE: Mass of the black hole.

RESULTS

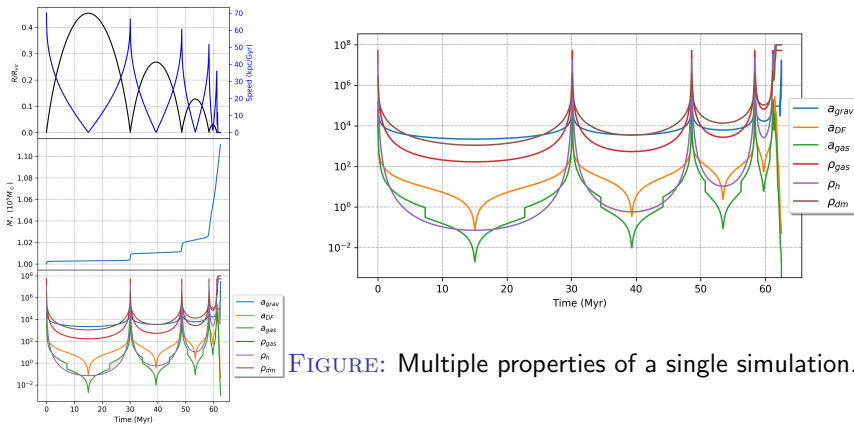


FIGURE: Multiple properties of a single simulation.

EFFECT OF THE POWER LAW EXPONENT

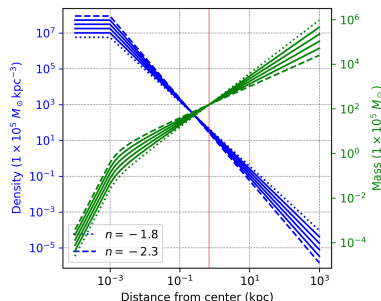
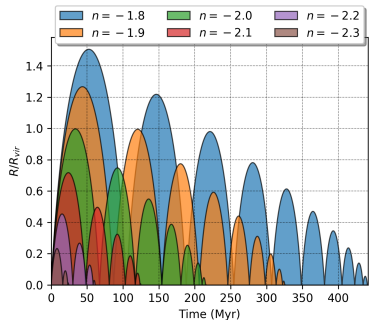


FIGURE: Smaller exponents increase the return time.

EFFECT OF THE BARYONIC FRACTION

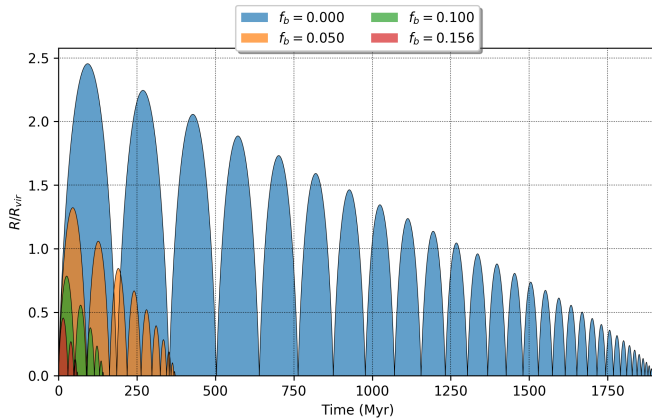


FIGURE: 5 % increase on baryonic fraction decreases return times.

EFFECT OF THE STELLAR FRACTION

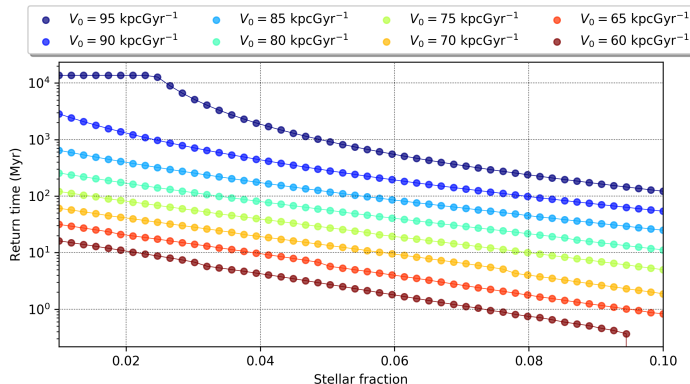


FIGURE: Return time for different stellar densities.

TRIAXIAL SETUP

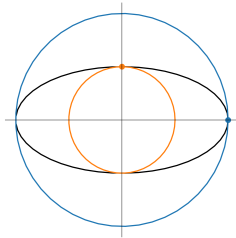


FIGURE: Effective gravitational mass

The contributions of all ellipsoidal shells that make up the profile are taken into account

$$\psi(m) \equiv \int_0^{m^2} \rho(m^2) dm^2 = \int_0^{k=m^2} \rho(k) dk \quad (9)$$

The potential of any body in which $\rho = \rho(m^2)$ is:

$$\Phi(\vec{x}) = -\pi G \frac{a_2 a_3}{a_1} \int_0^\infty \frac{\psi(\infty) - \psi(m)}{\sqrt{(\tau + a_1^2)(\tau + a_2^2)(\tau + a_3^2)}} d\tau \quad (10)$$

Numerical integration of the gradients of the potentials is made with Simpson 3/8 rule.

$$\nabla \Phi_{\text{DM}}(\vec{x}) = 2\pi G R_s^3 \rho_0 a_1 a_2 a_3 \int_0^\infty \frac{\vec{\phi}(\vec{x}, \tau) d\tau}{m(\vec{x}, \tau) (R_s + m(\vec{x}, \tau))^2} \quad (11)$$

$$\nabla \Phi_S(\vec{x}) = GM_s a_1 a_2 a_3 \int_0^\infty \frac{\vec{\phi}(\vec{x}, \tau) d\tau}{m(\vec{x}, \tau) (\mathcal{R}_f + m(\vec{x}, \tau))^3} \quad (12)$$

$$\nabla \Phi_G(\vec{x}) = 2\pi G \rho_0 a_1 a_2 a_3 \begin{cases} \int_0^\infty \vec{\phi}(\vec{x}, \tau) d\tau & \text{for } m(\vec{x}, \tau) < r_0 \\ r_0^{-n} \int_0^\infty m(\vec{x}, \tau)^n \vec{\phi}(\vec{x}, \tau) d\tau & \text{else} \end{cases} \quad (13)$$

RESULTS

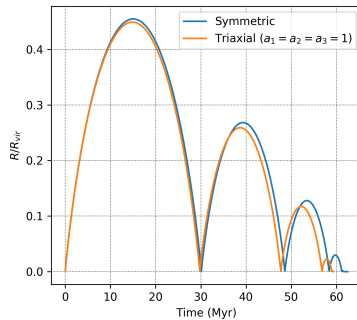
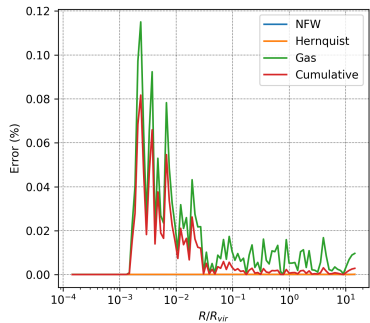


FIGURE: Differences for analytical and numerical integration of the potentials. Analytical is taken as: $-GM(r)/r^2$

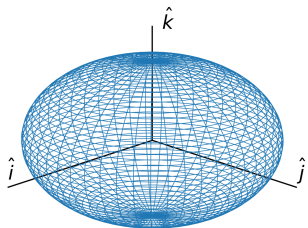
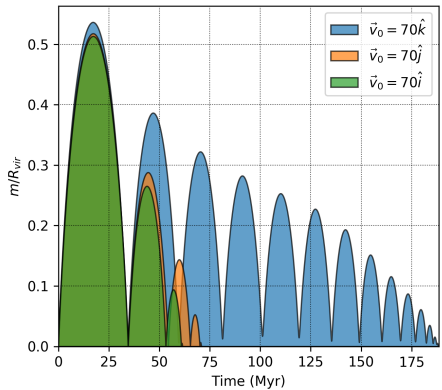


FIGURE: Orthogonal launches for a triaxial profile with semi-axis $(a_1:a_2:a_3) = (1:0.99:0.95)$

SCHEDULE

TABLE: Activity schedule

Activities	Week						
	1	2	3	4	5	6	7
Task 1	x						
Task 2	x	x					
Task 3		x	x	x			
Task 4					x	x	
Task 5							x

- Task 1:** REBOUND instalación in HPC ✓
- Task 2:** Understanding REBOUND examples ✓
- Task 3:** Implementation of a Choksi simulation ✓
- Task 4:** Implementation of a triaxial simulation ✓
- Task 5:** 30 % thesis dissertation ✓

SCHEDULE

TABLE: Activity schedule

Activities	Week								
	8	9	10	11	12	13	14	15	16
Task 6	x	x							
Task 7			x	x	x				
Task 8						x	x	x	x

Task 6: Optimization of the time step for *WHFast* y *IAS15*

Task 7: Implementation of an automated algorithm for the space of parameters of initial velocities and parameters of the triaxial potential, for the integrators *Leapfrog*, *WHFast* and *IAS15*

Task 8: Analysis and writing of the document

└ STUDIES
└ TRIAXIAL

THANK YOU

Computer simulations are sensitive to rounding errors due to the lack of infinite precision when representing decimal numbers.

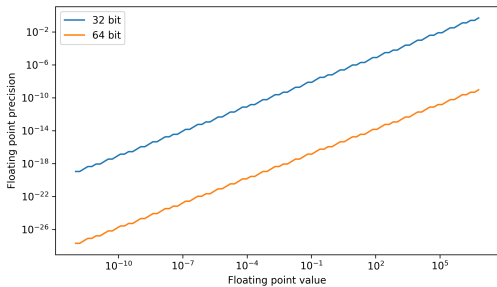


FIGURE: Floating point precision for different values, for a 32 bit and 64 bit holders.

Mass distributions between components are given by:

$$M_{\text{DM}}(R_{\text{vir}}) = (1 - f_b) M_h \quad (14)$$

$$M_{\text{stars}}(R_{\text{vir}}) = f_s f_b M_h \quad (15)$$

$$M_{\text{gas}}(R_{\text{vir}}) = (1 - f_s) f_b M_h \quad (16)$$

with $f_b = 0.156$ and $M_h = 10^8 M_\odot$

$$R_{\text{vir}} = \left(\frac{M_h G}{100 H(t)^2} \right)^{1/3} \quad (17)$$

DYNAMICAL FRICTION

As the black hole travels through the galaxy, dark matter, stars and gaseous materials from the medium interact with the black hole adding a drag force.

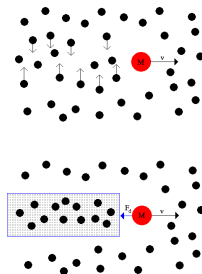


FIGURE: Collisionless dynamical friction

- Collisionless matter interacts with the black hole gravitational only

$$a_{\text{DF}}^{\text{cl}}(\vec{x}, \dot{\vec{x}}) = -\frac{4\pi G^2}{\dot{x}^2} M_\bullet \rho(\vec{x}) \ln \Lambda \left(\text{erf}(X) - \frac{2}{\sqrt{\pi}} X e^{-X^2} \right) \quad (18)$$

- On the other side gas is in direct contact with the black hole

$$a_{\text{DF}}^{\text{c}}(\vec{x}, \dot{\vec{x}}) = -\frac{4\pi G^2}{\dot{x}^2} M_\bullet \rho_{\text{gas}}(\vec{x}) f(\mathcal{M}) \quad (19)$$

ACCRETION INTO THE BLACK HOLE

As the black hole accretes matter from the surroundings, an acceleration appears, due to the second law of Newton.

$$\dot{M}_\bullet(\vec{x}, \dot{\vec{x}}) = \begin{cases} \dot{M}_\bullet^{\text{BHL}}(\vec{x}, \dot{\vec{x}}) & \text{if } \dot{M}_\bullet^{\text{BHL}} < \dot{M}_\bullet^{\text{Edd}} \\ \dot{M}_\bullet^{\text{Edd}} & \text{else} \end{cases} \quad (20)$$

$$\dot{M}_\bullet^{\text{BHL}}(\vec{x}, \dot{\vec{x}}) = \frac{4\pi G^2 \rho_G(\vec{x}) M_\bullet^2}{(c_s^2 + \dot{x}^2)^{3/2}} \quad (21)$$

$$\dot{M}_\bullet^{\text{Edd}} = \frac{(1 - \epsilon) M_\bullet}{\epsilon t_{\text{Edd}}} \quad \epsilon = 0.1, \quad t_{\text{Edd}} = 0.44 \text{ Gyr} \quad (22)$$

Drag generated by gas depends on local sound speed

$$\mathcal{M}(\dot{x}) \equiv \frac{|\dot{x}|}{c_s} = |\dot{x}| \sqrt{\frac{\mathcal{M}_w}{\gamma R T_{\text{vir}}}} = |\dot{x}| \sqrt{\frac{\mathcal{M}_w}{\gamma R} \left(\frac{2k_B R_{\text{vir}}}{\mu m_p G M_h} \right)} \quad (23)$$

$$\mathcal{M}(\dot{x}) = 1.63 |\dot{x}| \sqrt{\frac{R_{\text{vir}}}{M_h}}$$

$$a_{\text{DF}}^c(\vec{x}, \dot{\vec{x}}) = -\frac{4\pi G^2}{\dot{x}^2} M_\bullet \rho_{\text{gas}}(\vec{x}) f(\mathcal{M}) \quad (24)$$

with

$$f(\mathcal{M}) = \begin{cases} 0.5 \ln \Lambda \left[\operatorname{erf}\left(\frac{\mathcal{M}}{\sqrt{2}}\right) - \sqrt{\frac{2}{\pi}} \mathcal{M} e^{-\mathcal{M}^2/2} \right] & \text{if } \mathcal{M} \leq 0.8 \\ 1.5 \ln \Lambda \left[\operatorname{erf}\left(\frac{\mathcal{M}}{\sqrt{2}}\right) - \sqrt{\frac{2}{\pi}} \mathcal{M} e^{-\mathcal{M}^2/2} \right] & \text{if } 0.8 < \mathcal{M} \leq \mathcal{M}_{eq} \\ 0.5 \ln (1 - \mathcal{M}^{-2}) + \ln \Lambda & \text{if } \mathcal{M} > \mathcal{M}_{eq} \end{cases} \quad (25)$$

TRIAXIAL SETUP

Density shells for each profile are ellipsoids

$$m^2(\vec{x}) \equiv x_1^2 + \left(\frac{a_1}{a_2}\right)^2 x_2^2 + \left(\frac{a_1}{a_3}\right)^2 x_3^2 \quad (26)$$

A thin shell, whose inner and outer skins are the surfaces m and $m + \delta m$ is described by:

$$m^2(\vec{x}, \tau) = a_1^2 \left(\frac{x_1^2}{\tau + a_1^2} + \frac{x_2^2}{\tau + a_2^2} + \frac{x_3^2}{\tau + a_3^2} \right) \quad (27)$$

where $\tau \geq 0$ labels the surfaces

↘ STUDIES
 ↘ TRIAXIAL

$$\omega = \frac{\tau^\gamma}{\tau^\gamma + 1}, \quad \tau = \left(\frac{\omega}{1 - \omega} \right)^{\frac{1}{\gamma}}, \quad d\tau = \frac{\left(-\frac{\omega}{\omega - 1} \right)^{\frac{1}{\gamma}}}{\gamma \omega (-\omega + 1)} \quad (28)$$

$$\phi_i(x_i, \tau) = \frac{x_i}{(\tau + a_i^2)^{\frac{3}{2}} \prod_{i \neq j}^3 \sqrt{\tau + a_j^2}} \quad (29)$$

$$\vec{\phi}(\vec{x}, \tau) = (\phi_1(x_1, \tau), \phi_2(x_2, \tau), \phi_3(x_3, \tau)) \quad (30)$$